

Fermi National Accelerator Laboratory

FERMILAB-Conf-98/003-E

CDF

Calibration and Testing of the CDF II Endplug Calorimeter

S. Lusin

For the CDF Plug Upgrade Group

*University of Wisconsin
Madison, Wisconsin 53706*

*Fermi National Accelerator Laboratory
P.O. Box 500, Batavia, Illinois 60510*

January 1998

Published Proceedings of the *7th International Conference on Calorimetry in High-Energy Physics*,
Tucson, Arizona, November 9-14, 1997

Disclaimer

This report was prepared as an account of work sponsored by an agency of the United States Government. Neither the United States Government nor any agency thereof, nor any of their employees, makes any warranty, expressed or implied, or assumes any legal liability or responsibility for the accuracy, completeness, or usefulness of any information, apparatus, product, or process disclosed, or represents that its use would not infringe privately owned rights. Reference herein to any specific commercial product, process, or service by trade name, trademark, manufacturer, or otherwise, does not necessarily constitute or imply its endorsement, recommendation, or favoring by the United States Government or any agency thereof. The views and opinions of authors expressed herein do not necessarily state or reflect those of the United States Government or any agency thereof.

Distribution

Approved for public release; further dissemination unlimited.

CALIBRATION AND TESTING OF THE CDF II ENDPLUG CALORIMETER

S. LUSIN

*Department of Physics
University of Wisconsin
Madison, WI 53706, USA*

for the CDF Plug Upgrade Group^a

The CDF II End Plug Calorimeter is a sampling calorimeter based on plastic scintillating tiles using a projective tower geometry. The tiles are read out by wavelength-shifting fibers embedded in the tiles. A description of the CDF II End Plug Calorimeter is presented along with results from test beam and cosmic-ray testing taking place at Fermi National Accelerator Laboratory during the past year. The performance of the calorimeter is within the design specifications.

1 Introduction

The CDF II Endplug Calorimeter¹ is a sampling calorimeter based on scintillating tiles with fiber readout and projective tower geometry. It covers a pseudorapidity range of $1.1 < |\eta| < 3.6$ ($3^\circ < \theta < 37^\circ$) and will replace a gas calorimeter, which has a time response incompatible with expected rates during Run II at the Tevatron, where the time between bunch crossings may be as short as 132 ns.

The tower segmentation is approximately $0.1 \times 7.5^\circ$ in $\eta - \phi$ space. This choice of segmentation is motivated by the need for good efficiency in the e^\pm identification in semileptonic decays of b/\bar{b} jets while keeping the total number of channels within reasonable limits.

2 Detector Description

A one quadrant cross-sectional view of the CDF II End Plug Calorimeter is shown in figure 1. The calorimeter consists of two primary sections, the electromagnetic (EM) calorimeter and the hadronic calorimeter.

The EM calorimeter³ consists of 23 layers of 4mm thick plastic scintillator and 4.5mm lead plates with stainless-steel cladding. The first layer, however, consists of 10mm thick scintillator that is read out separately from the other

^aMembers of the following CDF institutions participate in the Plug Upgrade Project: University of Bologna, Brandeis University, Fermilab, KEK, Michigan State University, Purdue University, Rochester University, Rockefeller University, Texas Tech University, Tsukuba University, UCLA, University of Udine, Waseda University, and University of Wisconsin.

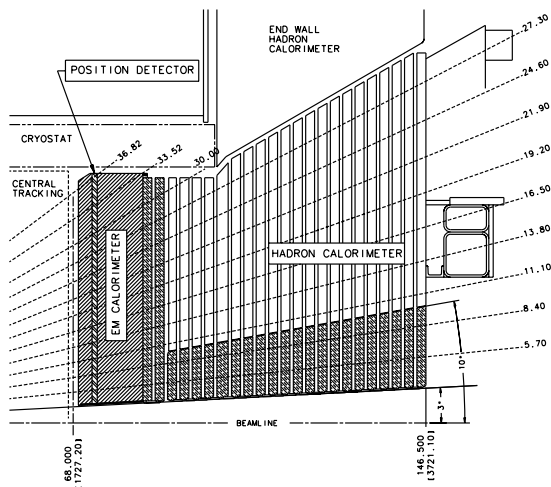


Figure 1: A one-quadrant cross-sectional view of the CDF II Endplug Calorimeter.

layers and is used as a preshower detector. Six radiation lengths into the EM calorimeter there is a shower maximum detector composed of crossed scintillating strips with fiber readout.

Behind the EM calorimeter is the hadronic calorimeter⁴, which consists of 6mm thick plastic scintillator and 2" thick steel absorber plates. This design reuses the steel of the previous calorimeter, with the addition of stainless steel plates welded into the 10° central hole.

The active elements of the calorimeter are scintillating tiles assembled into 15° modules called *megatiles*, which are shown in figure 2. The tiles are read out with a single turn of waveshifting fiber² spliced to a length of clear fiber that leads to an optical connector at the edge of the megatile.

From there, optical fibers carry the light to a temperature-controlled PMT box containing a “decoder” box which reorders the fibers from a megatile-wise bundling to a tower-wise bundling. Tower bundles are then routed to separate phototubes. A laser calibration system, not shown in the figure, can inject light through the decoder boxes and is used for setting initial PMT gains.

3 Design Requirements

The design parameters for the EM and hadronic calorimeters are listed in table 1. The requirements for calorimeter resolution were determined by simulation

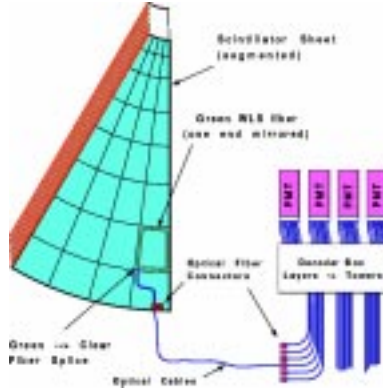


Figure 2: One 15° scintillating tile module and optical readout system for the endplug calorimeter.

studies. In the case of the EM calorimeter, the stochastic term, which is a function of the sampling fraction, must be $16\%/\sqrt{E}$ or less. The constant term, which is primarily a function of transverse uniformity, must be 1% or less. Nonlinearity, which is a function of longitudinal nonuniformity, must be 1% or less. In the case of the hadron calorimeter, the requirements are less stringent.

Table 1: Technical parameters and design specifications of the Plug Upgrade Calorimeter. The EM (HAD) resolution is for a single electron (pion).

| | EM | HAD |
|---------------------------|--------------------------------|----------------------------------|
| Segmentation | $\sim 8 \times 8 \text{ cm}^2$ | $\sim 24 \times 24 \text{ cm}^2$ |
| Total Channels | 960 | 864 |
| Thickness | $21 X_0, 1 \lambda_0$ | $7 \lambda_0$ |
| Density | $0.36 \rho_{Pb}$ | $0.75 \rho_{Fe}$ |
| Samples | 22 + Preshower | 22 |
| Active | 4 mm SCSN38 | 6 mm SCSN38 |
| Passive | 4.5 mm Pb | 2 inch Fe |
| Light Yield (pe/MIP/tile) | ≥ 3.5 | ≥ 2 |
| Non-linearity | $\leq 1 \%$ | 5-10 % |
| Resolution | $16\%/\sqrt{E} \oplus 1\%$ | $80\%/\sqrt{E} \oplus 5\%$ |

In order to meet these conditions, the following requirements were placed on the tiles and optical fibers: to meet the stochastic term requirement in

the EM (HAD) resolution, the light yield must be better than 3.5 (2) photo-electrons/MIP/tile; to meet the constant term requirement in the EM (HAD) resolution, the transverse uniformity of tile response must have an $\text{r.m.s} < 2.5\%$ (4%); and to meet the EM (HAD) linearity requirement, the longitudinal uniformity of tile response must have an $\text{r.m.s} < 10\%$ (10%). These requirements were used to set the Quality Assessment (QA) parameters during the manufacture of the tiles and fibers.

4 Test Beam Results

A model of the calorimeter, equivalent to a 45° section of the EM calorimeter mounted on a 60° section of the hadronic calorimeter was constructed and its performance measured at the Fermilab Meson Beam Line.

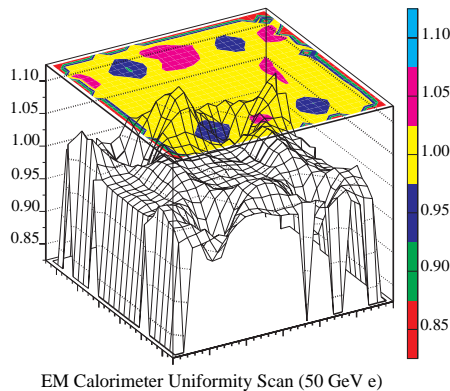


Figure 3: Results of an electron beam position scan across the face of an EM tower.

Shown in figure 4 are the results of a measurement of EM calorimeter response to a 55 GeV electron beam, as the beam was scanned across the face of a calorimeter tower. The results are presented as a two-dimensional surface plot with a contour projection above. There are four “cold” spots, corresponding to the tower corners, and a “hot” spot, corresponding to the location of a section of wavelength shifting fiber. In both of these cases, the deviation is only 5% away from the average response. Overall, the r.m.s spreads in the transverse uniformity for the EM and hadronic calorimeters are 1.6% and 2.3%, respectively, which are within the design requirements.

Overall, the End Plug Calorimeter meets or exceeds the design requirements. Figure 4 shows the results of an electron beam energy scan. The

stochastic and constant terms are measured to be $14.5\%/\sqrt{E}$ and 0.7% , respectively.

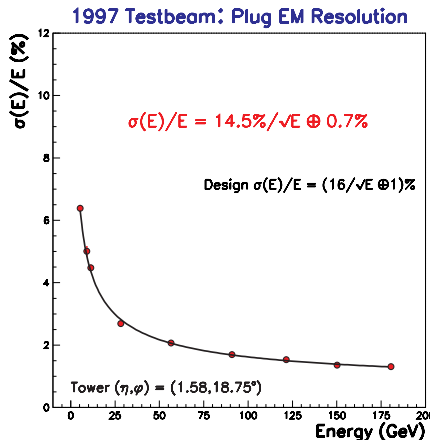


Figure 4: Results of an electron beam energy scan.

Results from beam tests show that EM linearity meets the 1% requirement, both in the case where the EM calorimeter is exposed directly to an electron beam and in the case where 1.5 radiation lengths of material are placed in front of the calorimeter to approximate the effects of the central tracker endplate and the silicon vertex detector, and then correcting for energy deposited before the calorimeter by using preshower information.

5 Monitoring and Calibration System

The laser calibration system⁶ is used to set the initial PMT gains and to monitor the stability of the PMTs. Once the PMT gains have been equalized, the residual spread in the tower response to e^+ and μ^+ is $\sim 5\%$ r.m.s.

In addition to the laser system, a system using a Cs^{137} movable radioactive source⁵ that can expose each tile individually is used for further refinement of the tower responses, and as a reference for energy scale determination.

Figure 5 shows the correlation between the response of the towers to the Cs^{137} source and to 55 GeV e^+ , and shows that the wire source system can be used to achieve a level of response uniformity of $\sim 1.8\%$ r.m.s.

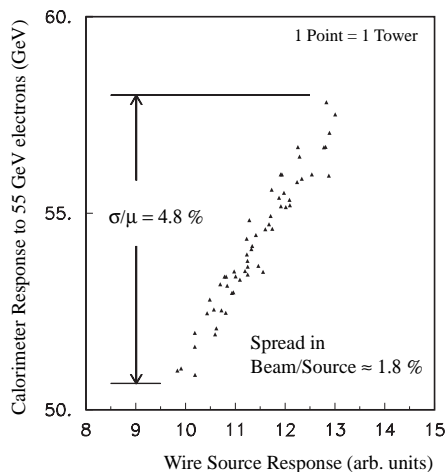


Figure 5: The correlation of electron response with wire source current.

6 Cosmic Ray Testing

In addition to the calorimeter model built for the beam test, a cosmic ray test stand was built for the purpose of testing the entire EM calorimeter. A cosmic ray test of the entire EM calorimeter will provide us with an initial calibration and will test every tower prior to detector installation.

The test stand consists of a support table of 10" thick steel, which acts as a hardener, on which the calorimeter is placed, with the "beam axis" vertical. There are wire chambers above and below the calorimeter for tracking cosmic ray muons. The tracking chambers provide coverage for only one quadrant of the calorimeter at a time. The calorimeter is lifted and rotated to expose successive quadrants. There are two planes of trigger counters, above and below the upper tracking chamber. Additional trigger information is obtained from the lower chamber.

Figure 6 shows the ADC spectrum of a particular EM tower during a cosmic ray test. The light shaded region represents the ADC response of a particular tower to all cosmic ray triggers for projective tracks, and shows a large pedestal peak. The dark shaded region corresponds to the ADC response of the same tower for those events in which a cosmic ray track falls within the fiducial region of the calorimeter tower, and shows a strong suppression of the pedestal peak (although there is some leakage.) The muon peak is clearly visible above the pedestal.

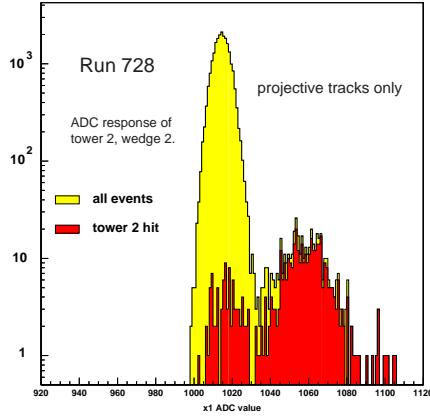


Figure 6: The ADC response of a calorimeter tower. The dark shaded region corresponds to those events where a cosmic ray track falls within the fiducial region of the calorimeter tower.

The uniformity of tower response to cosmic ray muons is in agreement with that of e^+ and μ^+ response for the test beam module. Figure 7 shows the distribution of mean values of the muon peak for towers with a fully contained track. A $\cos\theta$ -dependent path length correction has been applied to the ADC values prior to fitting for the muon peak position. The spread in the tower response is 1.9% r.m.s., which approaches the limit of uniformity achievable with the Cs^{137} source calibration system.

Acknowledgments

Work supported in part by U.S. DOE under contract No. DE-FG02-95ER40896

References

1. G. Apollinari *et al.*, in *Proceedings of the Fourth International Conference on Calorimetry in High Energy Physics*, La Biodola, Italy, ed. A. Menzione *et al.* (World Scientific, Singapore, 1993), p. 200
2. J. P. Mansour *et al.*, in *Proceedings of the Workshop on Scintillating Fiber Detectors*, Notre Dame, Indiana, ed. A. D. Bross *et al.* (World Scientific, Singapore, 1993), p. 534

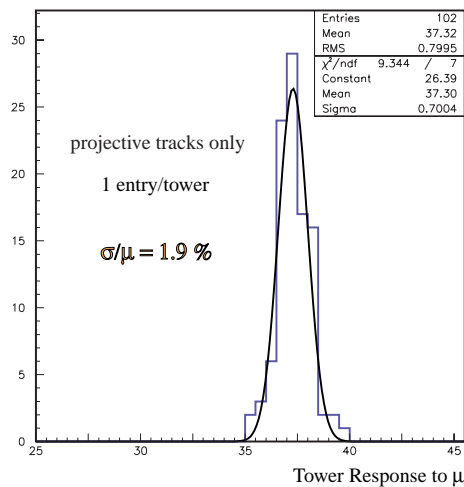


Figure 7: The distribution of muon peak mean positions for the EM calorimeter under cosmic ray testing. Data from one calorimeter quadrant is shown.

- G. Apollinari *et al.*, *Nucl. Instrum. Methods A* **311**, 520 (1992)
- 3. T. Asakawa *et al.*, *Nucl. Instrum. Methods A* **340**, 458 (1994)
- S. Aota *et al.*, *Nucl. Instrum. Methods A* **352**, 557 (1995)
- 4. P. de Barbaro *et al.*, *IEEE Trans. Nucl. Sci.* **42**, 510 (1995)
- 5. V. Barnes *et al.*, in *Proceedings of the First International Conference on Calorimetry in High Energy Physics*, Batavia, Illinois, ed. D. F. Anderson *et al.* (World Scientific, Singapore, 1990), p. 189
- 6. D. Cauz *et al.*, in *Proceedings of the Sixth International Conference on Calorimetry in High Energy Physics*, Frascati, Italy, ed. A. Antonelli *et al.* (Frascati Physics Series, 1996), p. 369